

PAPER • OPEN ACCESS

Structural and morphological properties of sol-gel ZnO:Ni films

To cite this article: T Ivanova *et al* 2018 *J. Phys.: Conf. Ser.* **992** 012044

View the [article online](#) for updates and enhancements.

Related content

- [Influence of bone morphological properties on a new expandable orthopaedic fastener](#)
M Oldakowski, I Oldakowska, T B Kirk et al.
- [Study of post annealing effects on structural and optical properties of sol-gel derived ZnO thin films grown on n-Si substrate](#)
Aniruddh Bahadur Yadav, C Periasamy and S Jit
- [Mechanical activation influence on the morphological properties of La₂O₃-TiO₂-B](#)
O Dolmatov, V Zakusilov, M Kuznetsov et al.

Structural and morphological properties of sol-gel ZnO:Ni films

T Ivanova^{1,5}, A Harizanova¹, T Koutzarova², B Vertruyen³ and B Stefanov⁴

¹Central Laboratory of Solar Energy and New Energy Sources,
Bulgarian Academy of Sciences, 72 Tzarigradsko Chaussee, 1784 Sofia, Bulgaria

²E. Djakov Institute of Electronics, Bulgarian Academy of Sciences,
72 Tzarigradsko Chaussee, 1784 Sofia, Bulgaria

³LCIS/SUPRATECS, Institute of Chemistry B6, University of Liege,
Sart-Tilman, B-4000 Liege, Belgium

⁴Department of Engineering Sciences, The Ångström Laboratory, Uppsala University,
P.O. Box 534, Uppsala, Sweden

E-mail: tativan@phys.bas.bg

Abstract. Ni doping induces modifications and considerable changes in the optical, electrical and magnetic properties of ZnO films. In this work, the influence is discussed of Ni-doping (two nickel concentrations) and annealing temperature (ranging from 300 °C to 800 °C) on the structural and optical properties of sol-gel derived ZnO:Ni films. Uniform and smooth films were obtained by spin-coating on quartz and Si substrates. The ZnO:Ni films were crystallized in wurtzite phase with no impurity phases found for annealing temperatures up to 600 °C. The size of the crystallites was strongly affected by the Ni content and the heat treatment. Furthermore, the Ni doping improved the optical transparency of the sol-gel films, while the AFM studies showed that the film morphology and the roughness were influenced by the nickel doping.

1. Introduction

ZnO is considered as being one of the most important semiconductors due to its wide bandgap (3.37 eV), large exciton energy (60 meV), thermal and chemical stability and hexagonal crystal structure. The ZnO nanostructured films possess desirable optical, structural and electronic properties for applications in thin-film transistors, solar cells, gas sensors, UV light emitting diodes, field emitters, piezoelectric devices, photo detectors, flat screen displays, sun screens, spintronic devices, etc. [1].

Doping the ZnO films modulates and changes their morphology, density of states, transmittance, bandgap, electrical conductivity, etc. [2]. Nickel is an important dopant, as Ni²⁺ has an ionic radius of 0.069 nm, which is slightly smaller than that of the Zn²⁺ ion (0.074 nm); thus, Ni²⁺ ions should be able to substitute Zn²⁺ in a ZnO matrix. ZnO:Ni films are being studied for potential applications in solar cells and memory devices [3]. Ni doping is a viable method of improving the sensing ability of ZnO by tuning the electronic band structure and modifying its energy levels and surface states. Since gas sensing is a surface phenomenon, where the sensing element's energy band bends upwards or

⁵ To whom any correspondence should be addressed.



downwards based on its interaction with an oxidizing or reducing gas, Ni can enhance the gas sensing properties [4]. ZnO films doped with Co, Ni, Fe have been widely studied as diluted magnetic semiconductors (DMS) [5]. Doped ZnO films exhibit magnetic behavior due to doping with transition metals and/or manifest magnetic properties through structural defects caused during the doped films' synthesis. The origin of ferromagnetism in nanostructured DMO's is still being explored and discussed [6].

ZnO doped films are deposited by pulse laser deposition, r.f. magnetron sputtering, molecular-beam epitaxy, CVD and ALD [7]. Among these methods, the sol-gel deposition has several advantages, such as inexpensive equipment, precise microstructural and chemical control, reproducibility, possibilities of engineering the films' properties. Preparation of high-quality ZnO-based nanostructured films by the sol-gel technology has been reported earlier [8].

In the present work, the effect is studied of adding Ni (two Ni concentrations) and varying the annealing temperature (300 °C – 800 °C) on the structural, optical and morphological properties of sol-gel Ni-doped ZnO films.

2. Experimental

The preparation of sols for ZnO and nickel-doped ZnO deposition were described previously [9]. Briefly, 0.4 M Zn sol and 0.2 M Ni sol were mixed in two volume ratios: ZnO:Ni 0.4 (19.6 ml Zn sol:0.4 ml Ni sol) and ZnO:Ni 1 (19 ml Zn sol :1 ml Ni sol). The films were obtained by spin coating at 4000 rpm on Si and quartz substrates. The layer deposition procedure was repeated five times with pre-heating of 300 °C/10 min between layers. The ZnO:Ni films were annealed at temperatures ranging from 300 °C to 800 °C.

A Bruker D8 XRD diffractometer (grazing angle 2°, step time 8 s) was used for the structural study. The FTIR spectra were taken by an IRPrestige-21 Shimadzu FTIR Spectrophotometer. The optical measurements were carried out by a Shimadzu 3600 UV-VIS spectrophotometer. The atomic force microscopy (AFM) observation was performed by employing a PSIA XE150 SPM/AFM instrument equipped with an ACTA silicon cantilever (AppNano), a tip radius 6 – 10 nm operating in non-contact mode.

3. Results and discussions

The XRD patterns of ZnO and ZnO:Ni films annealed at 300 °C and 600 °C are presented in figure 1; as seen, the annealing temperature influences significantly the crystallization behavior of ZnO-based films. The undoped ZnO films improve their crystallization gradually as the annealing temperature is raised. The Ni-doped ZnO films exhibit a more complicated crystallization evolution. ZnO:Ni 0.4 and ZnO:Ni 1 films manifest an enhanced crystallinity for the annealing temperatures of 300 °C, 400 °C and 500°C; then the crystallization degree deteriorates after the high-temperature treatment at 600 °C.

Our earlier studies [9] revealed that the ZnO:Ni 0.4 films achieved the best crystallization after treatment at 700 °C, while the ZnO:Ni 1 films exhibited the most intense XRD peaks after annealing at 800 °C.; or, doping with Ni affects significantly the crystallization behavior of ZnO:Ni films. For the

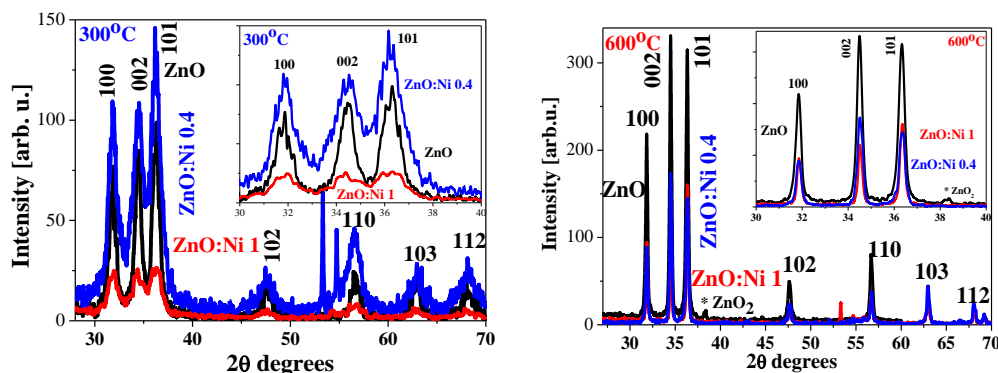


Figure 1. XRD patterns of ZnO, ZnO:In 0.4 and ZnO:Ni 1 films treated at 300 and 600°C.

films annealed at 300 °C (figure 1), the smaller Ni concentration induces a film crystallization comparable to that of the ZnO film, as the ZnO:Ni 1 films manifest weaker and broader XRD peaks, a sign of a less crystallized structure and possible traces of an amorphous phase. After annealing at 600 °C, the ZnO:Ni 0.4 and ZnO:Ni 1 films show lower crystallization compared to undoped ZnO films. The ZnO:Ni 0.4 and ZnO:Ni 1 films are polycrystalline, with all XRD peaks observed in their XRD patterns attributed to a hexagonal wurtzite phase of ZnO (according to JCPDS 01-07-8070) regardless of the annealing temperature, from 300 °C to 600 °C. No diffraction reflections assignable to Ni oxides or mixed Zn-Ni fractions are registered within the XRD detection limits. The ZnO:Ni 1 film treated at 800 °C reveals a broad peak at $2\theta = 43.2^\circ$ related to NiO bunsenite (JCPDS 00-004-0835) [9]. The presence of a NiO fraction indicates that the solubility of Ni in ZnO matrix is limited and dependent on the deposition method [10].

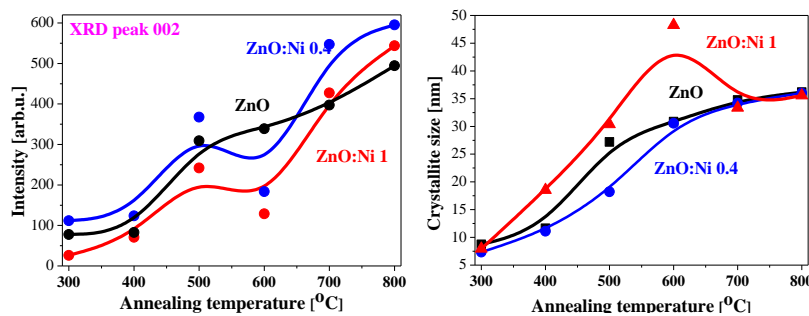


Figure 2. Intensity of the 002 main XRD peak and estimated crystallite size for ZnO and ZnO:Ni films depending on the annealing temperatures.

Figure 2 presents the annealing dependence of the 002 peak's XRD intensity and of the average crystallite size as estimated from the XRD peaks (100, 002 and 101 reflections) by using Scherrer's formula. It is seen that the XRD intensity depends strongly on the annealing temperature. The crystallites grow bigger as the annealing temperature is raised up to 600 °C for both the ZnO and ZnO:Ni films. After annealing at 700 °C and 800 °C, the ZnO:Ni crystallites grow smaller, their sizes become comparable to those of the ZnO films treated at these temperatures. The XRD analysis leads to the conclusion that Ni doping results in improved film crystallinity. The higher doping concentration (ZnO:Ni 1 films) leads to narrower XRD lines, i.e., greater crystallites compared to those of the ZnO and ZnO:Ni 0.4 films.

We further conducted FTIR measurements to examine the effect of Ni doping on the vibrational properties of sol-gel ZnO films; the results are shown in figure 3.

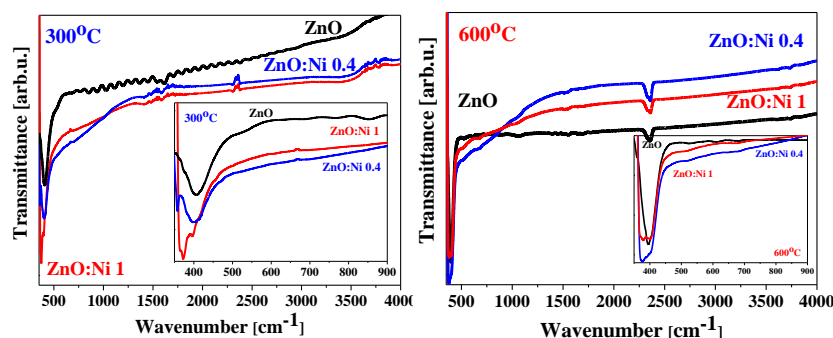


Figure 3. FTIR spectra of ZnO and ZnO:Ni films treated at 300 °C and 600 °C.

Metal-oxygen characteristic absorptions are exhibited in the fingerprint region below 1000 cm^{-1} . Absorptions due to organic residues and water inclusions appear above 1000 cm^{-1} . The ZnO:Ni films annealed at 300 °C show clear absorptions at 3780 cm^{-1} (adsorbed water molecules [11]) and broad bands near 3450 cm^{-1} (O-H stretching vibrations [12]). The ZnO film reveals a weak line at 3450 cm^{-1} . These bands vanish after high-temperature annealing. The weak band at 1640 cm^{-1} is assigned to the

bending $\delta(\text{HOH})$ vibration (seen in ZnO, ZnO:Ni films). The peak (seen in all spectra) at 2370 cm^{-1} is due to CO_2 absorbed from the atmosphere [13]. The absorption bands below 1000 cm^{-1} of the ZnO films annealed at $300\text{ }^\circ\text{C}$ are located at 760 cm^{-1} (due to Zn-O), 520 cm^{-1} (corresponding to wurtzite ZnO), and a very strong and broad line at 407 cm^{-1} with a shoulder at 370 cm^{-1} . The absorption bands at 407 cm^{-1} and 520 cm^{-1} are active infrared modes that have been confirmed theoretically for wurtzite ZnO [14]. The main absorption line of the ZnO:Ni 0.4 film centered at 402 cm^{-1} is very strong and broad with an additional peak at 360 cm^{-1} . Increasing the nickel content (ZnO:Ni 1) results in a modification of the main absorption feature: the band is located at 372 cm^{-1} with two lines at 396 cm^{-1} and 367 cm^{-1} . Annealing at $600\text{ }^\circ\text{C}$ induces stronger main absorption bands, shifted to 395 cm^{-1} (ZnO) and 376 cm^{-1} for the ZnO:Ni films. Weak lines at 680 cm^{-1} and 520 cm^{-1} are detected for all films. Adding Ni clearly results in a broadening of the absorption bands. The shifting to the infrared frequencies as the amount of the Ni^{2+} dopant is increased may be due to a difference in the bond length, which confirms the incorporation of Ni^{2+} in the ZnO lattice [15]. The absorption bands broadness can also point to a nanocrystalline nature of the films [12]. The FTIR studies did not indicate a presence of Ni oxide phases. This conclusion is in accordance with the XRD characterization.

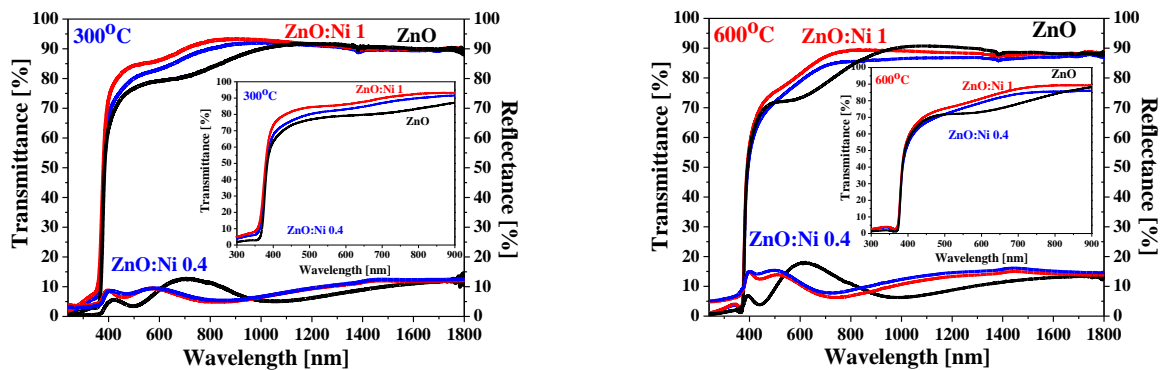


Figure 4. Transmittance and reflectance spectra of ZnO, ZnO:Ni films treated at $300\text{ }^\circ\text{C}$ and $600\text{ }^\circ\text{C}$.

Figure 4 presents a comparison of the optical spectra of ZnO and ZnO:Ni films. The estimated values of the optical bandgap (E_g) and the transmittance at 550 nm are given in table 1. Increasing the Ni doping improves the transparency, the reflectance being below 15% for the ZnO:Ni films. The transmittance reaches up to $80 - 84\%$ for the sol-gel ZnO:Ni 1 films.

The ZnO films' thickness was found to be 160 nm . The film thicknesses of the ZnO:Ni 0.4 and ZnO:Ni 1 films are 150 nm and 140 nm , respectively. The difference in the thickness of the films studied was small and thus, the optical properties could be compared.

The transparency of ZnO and ZnO:Ni films worsened with the temperatures, which became more pronounced after the treatments at $700\text{ }^\circ\text{C}$ and $800\text{ }^\circ\text{C}$. The optical bandgap values diminished as the annealing temperatures was increased, due to the bigger crystallite sizes. The optical bandgaps of

Table 1. Optical bandgap values, transmittance at $\lambda = 550\text{ nm}$ for ZnO and ZnO:Ni films as a function of the annealing temperatures.

$T_{\text{Annealing}} [^\circ\text{C}]$	ZnO	ZnO/NiO 0.4	ZnO/NiO 1	ZnO	ZnO/NiO 0.4	ZnO/NiO 1
	$E_g [\text{eV}]$			$T [\%] \text{ at } \lambda=550\text{ nm}$		
300°C	3,29	3,31	3,32	78,4	81,9	85,2
400°C	3,29	3,29	3,29	80,2	82,0	84,1
500°C	3,28	3,27	3,28	75,3	78,1	82,5
600°C	3,27	3,28	3,28	72,3	75,5	78,1
700°C	3,28	3,28	3,28	67,0	72,1	77,9
800°C	3,27	3,28	3,28	65,6	73,6	74,6

ZnO:Ni films are slightly higher than the corresponding ZnO values. The estimated E_g values are within the range of the data reported previously [4, 16].

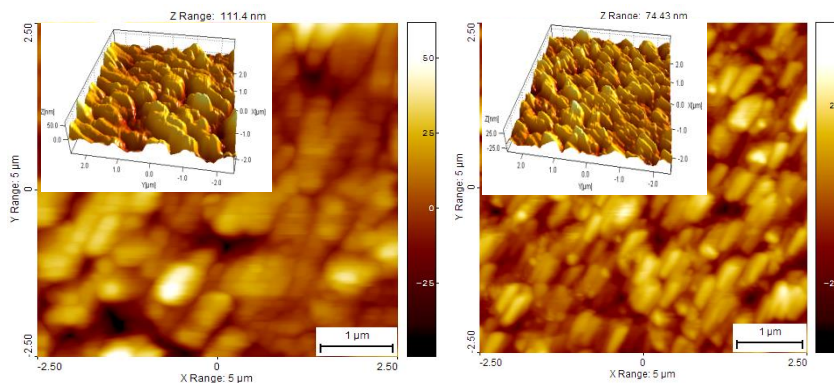


Figure 5. AFM micrographs of ZnO:Ni 0.4 and ZnO:Ni 1 films treated at 600 °C. The inset images are 3D micrographs.

Figure 5 presents AFM micrographs of the ZnO:Ni 0.4 and ZnO:Ni 1 films treated at 600 °C (scan area of 5×5 μm). The AFM study of a ZnO film performed at a scan area of 2×2 μm reveals a smooth and uniform morphology with a grained film structure and an uneven size distribution. The grains are well-packed, which results in a small r.m.s. roughness $R_q = 5.115$ nm for the undoped ZnO film (not shown here). It is known that the roughness parameters are higher when the scan area is increased, because longer-wavelength topography components are then sampled [17]. Thus, direct comparison with the results for the ZnO:Ni films cannot be done. The AFM micrographs of the ZnO:Ni films show different morphological features. Their average and r.m.s. roughness is given in Table 2. The ZnO:Ni 0.4 film shows bigger grains with greater heights compared to the ZnO:Ni 1 films (see 3D images, figure 5). On the other hand, the XRD analysis reveals that the ZnO:Ni 0.4 film annealed at 600 °C possesses smaller crystallites compared to ZnO:Ni 1, which can be a sign of micro-strain broadening of the XRD peaks.

Table 2. AFM parameters of sol-gel ZnO, ZnO:Ni 0.4 and ZnO:Ni 1 films treated at 600°C.

AFM parameter	ZnO (2x2 μm)	ZnO:Ni 0.4 (5x5 μm)	ZnO:Ni 1 (5x5 μm)
Average roughness	4,215	8,246	7,00
r.m.s. roughness	5,115	10,368	8,455

ZnO:Ni 1 shows lower roughness parameters values, indicating a smoother surface with a closely-packed granular structure. This may explain its improved transparency. On the other hand, due to its rougher surface and, hence, more intensive light scattering, the ZnO:Ni 0.4 films exhibit a lower transmittance in the visible range. The conclusion we draw from the AFM study is that Ni-doping affect substantially the film surface morphology.

4. Conclusions

The work presented demonstrates that the sol-gel approach is a successful simple technology for depositing Ni-doped ZnO films. The ZnO:Ni films thus prepared are uniform, smooth, and polycrystalline with a wurtzite crystal phase. The FTIR analysis shows that Ni-doping changes the characteristic light absorption features. The transparency is improved by Ni incorporation and the optical bandgap of the ZnO:Ni films is slightly wider than that for ZnO films.

References

- [1] Muniyandi I, Mani G K, Shankar P and Rayappan J B B 2014 *Ceramics Inter.* **40** 7993
- [2] Chaitra U, Kekuda D and Rao K M 2017 *Ceramics Inter.* **43** 7115
- [3] Kayani Z N, Naz F, Riaz S and Naseem Sh 2017 *J. Saudi Chem. Soc.* **21** 425

- [4] Mani G K and Rayappan J B B 2014 *Appl. Surf. Sci.* **311** 405
- [5] Ramesh J, Pasupathi G, Mariappan R, Kumar V S and Ponnuswamy V 2013 *Optik* **124** 2023
- [6] Montes-Valenzuela I, Romero-Paredes G, Vázquez-Agustín M A, Baca-Arroyo R and Peña-Sierra R 2015 *Mater. Sci. Semicond. Processing* **37** 185
- [7] Siddheswaran R, Netrvalová M, Savková J, Novák P, Očenášek P, Šutta P, Kováč Jr J and Jayavel R 2015 *J. Alloys Comp.* **636** 85
- [8] Srinet G, Kumar R and Sajal V 2013 *J. Appl. Phys.* **114** 033912
- [9] Ivanova T, Harizanova A, Koutzarova T and Vertruyen B 2015 *Proc. 15th Int. Conf. Nanotechnol. (IEEE-NANO 2015)* **7388970** 250
- [10] Goswami N and Sahai A 2013 *Mat. Res. Bulletin* **48** 346
- [11] Tang A, Li X, Zhou Zh, Ouyang J and Yang H 2014 *J. Alloys Comp.* **600** 204
- [12] El-Kemary M, Nagy N and El-Mehasse I 2013 *Mater. Sci. Semicond. Processing* **16** 1747
- [13] Malika A N, Reddy A R, Babu K S and Reddy K V 2014 *Ceramics Int.* **40** 12171
- [14] Iordanescu C, Tenciu D, Feraru I, Kiss A, Bercu M, Savastru D, Notonier R and Grigoresc C 2001 *Digest J. Nanomater. Biostr.* **6** 863
- [15] Shinde K P, Pawar R C, Sinha B B, Kim H, Oh S and Chung K C 2014 *Ceramics Int.* **40** 16
- [16] Xu K, Liu C, Chen R, Fang X, Wu X and Liu J 2016 *Physica B: Cond. Matter* **502** 155
- [17] Elam J W, Sechrist Z A and George S M 2012 *Thin Solid Films* **414** 43